

# The Origin of Quarks in Quantum Gravity

Edwin Eugene Klingman 

Cybernetic Micro Systems, Inc., San Gregorio, USA

Email: [klingman@geneman.com](mailto:klingman@geneman.com)

**How to cite this paper:** Klingman, E.E. (2024) The Origin of Quarks in Quantum Gravity. *Journal of Modern Physics*, 15, 1229-1245.

<https://doi.org/10.4236/jmp.2024.158050>

**Received:** June 8, 2024

**Accepted:** July 26, 2024

**Published:** July 29, 2024

Copyright © 2024 by author(s) and Scientific Research Publishing Inc. This work is licensed under the Creative Commons Attribution International License (CC BY 4.0).

<http://creativecommons.org/licenses/by/4.0/>



Open Access

---

## Abstract

A theory of quantum gravity has recently been developed by the author based on the concept that all forces converge to one at the moment of Creation. This primordial field can only interact with itself, as no other field exists, contrasting with the Standard Model of Particle Physics in which each elementary particle is an excitation in its own quantum field. The primordial field theory of quantum gravity has produced a model of a fermion with a mass gap,  $\frac{1}{2}$ -integral spin, discrete charge, and magnetic moment. The mass gap is based on an existence theorem that is anchored in Yang-Mills, while Calabi-Yau anchors  $\frac{1}{2}$ -integral spin, with charge and magnetic moment based on duality. Based on  $N$ -windings, this work is here extended to encompass fractional charge, with the result applied to quarks, yielding fermion mass and charge in agreement with experiment and novel size correlations and a unique quantum gravity-based ontological understanding of quarks.

## Keywords

Duality, Calabi-Yau Topology, Fermion Charge, Primordial Field, Self-Interaction Equations, Yang-Mills Gravity, Quantum Gravity, Ontology of Quarks

---

## 1. Introduction

Since at least 1974 physicists have considered mesons and baryons to consist of quarks; the origin of such is still mysterious. Quarks are never observed individually, and this has done little to remove the mystery. When combined with the variety of approaches to quantum gravity, and the singular lack of results from this field [1], it seems reasonable to consider new approaches. For example, Nilsen has hypothesized a triotron particle that annihilates electrons and positrons and uses these to formulate his concept of electrons and quarks [2]. Singh [3] has adapted the idea of “spontaneous collapse” proposed by Ghirardi, Rimini, Weber, and Pearle (GRWP) to spontaneous quantum gravity. We will briefly summarize these approaches after developing an approach developed by the au-

thor based on a primordial field theory, in which all interaction is self-interaction, due to the simple fact that, in the beginning, no other field exists with which to interact.

If this self-interaction equation is formulated in the usual manner, we obtain the master equation

$$\nabla \psi = \psi \psi \tag{1}$$

where  $\nabla$  is the difference operator acting on the field  $\psi$ , assumed equivalent to the local field interacting with itself. If one employs Hestenes' Geometric Calculus, wherein  $ab = a \cdot b + a \wedge b$  and duality operation  $a \wedge b = -i(a \times b)$  and one assumes  $\psi = \mathbf{G} + i\mathbf{C}$  and  $\nabla = \nabla + i\partial_t$ , so Equation (1) becomes

$$(\nabla + \partial_t)(\mathbf{G} + i\mathbf{C}) = (\mathbf{G} + i\mathbf{C})(\mathbf{G} + i\mathbf{C}) \tag{2}$$

and the expansion results in terms containing  $\mathbf{G} \cdot \mathbf{G}$ ,  $\mathbf{C} \cdot \mathbf{C}$ , and  $\mathbf{G} \cdot \mathbf{C}$ , as well as derivative terms based on  $\nabla$  and  $i\partial_t$ . Since  $\mathbf{G}$  and  $\mathbf{C}$  are orthogonal fields, we assume  $\mathbf{G} \cdot \mathbf{C} = \mathbf{C} \cdot \mathbf{G} \equiv 0$ , and further assume that  $\mathbf{G} \cdot \mathbf{G}$  and  $\mathbf{C} \cdot \mathbf{C}$  are proportional to energy density of the  $\mathbf{G}$  and  $\mathbf{C}$  fields, with  $\mathbf{G} \times \mathbf{C}$  resembling a Poynting vector interpreted as momentum density vector. Grouping like terms and re-expressing the equations in terms of mass density  $\rho = \mathbf{G} \cdot \mathbf{G} + \mathbf{C} \cdot \mathbf{C}$  and  $\rho \mathbf{v} \sim \mathbf{G} \times \mathbf{C}$  the self-interaction equation becomes the Heaviside equations for gravitomagnetism.

$$\begin{aligned} \nabla \cdot \mathbf{G} &= -\rho & \nabla \cdot \mathbf{C} &= 0 \\ \nabla \times \mathbf{C} &= -\rho \mathbf{v} + \partial_t \mathbf{G} & \nabla \times \mathbf{G} &= -\partial_t \mathbf{C} \end{aligned} \tag{3}$$

In "Particle Creation from Yang-Mills" [4] I analyze the Yang-Mills non-abelian term describing self-interaction and conclude that it does not make much physical sense. Instead, the gauge field interaction with itself  $[A_\mu, A_\nu]$  is replaced by dynamic term  $[A_\mu^{(i)}, A_\mu^{(i+2)}]$  representing self-interaction of higher order self-interaction fields. A fractal lattice was constructed, and path integrals were defined on this lattice; this treatment shows that these self-interactions reach a self-stabilizing zone that leads to a shrinking torus, consistent with earlier analysis of self-linked structures.

Jefimenko [5] showed that gravitomagnetism is dual to Maxwellian electromagnetism when mass does not depend upon velocity. This, and the scale-free nature of the self-interaction principle, imply that dual structures exist, as depicted by the dual  $U(1) \times U(1)$ -symmetry in Figure 1.

## 2. Comparison with Quantum Field Theory

How does *primordial field theory* (PFT) compare with *quantum field theory* (QFT)? We began with primordial field  $\psi$ , which has two aspects  $\mathbf{G}$  and  $i\mathbf{C}$  satisfying Heaviside's equation and interacts only with itself [6]. In *quantum field theory* a separate field exists for each and every type of particle in the "particle zoo". QFT fields, when stimulated, produce, or create, a particle of the appropriate type, which travels until it encounters another particle (of any type)

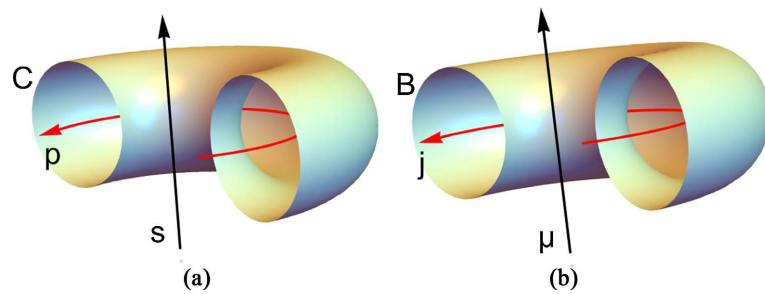


**Figure 1.** (a) Gravitomagnetic structure: momentum density  $p$ , field  $C$  and spin  $s$ ; (b) Electrodynamic dual: electric current density  $j$ , field  $B$ , and magnetic moment  $\mu$ .

with which it interacts. This is essentially the “mattress model” which is envisioned as a 2D lattice of point masses connected to each other by springs. Jumping on the mattress at a point stimulates excitations that travel along the springs, interacting with other such excitations. Zee [7] noted that, almost 100 years later, QFT remains rooted in this harmonic paradigm, and remarked that string theory is also founded on this harmonic paradigm. String theory has still produced no results and QFT, while providing a statistical theory of many particle physics, has not provided fundamental understanding of particles. These facts suggest that new approaches be investigated, and primordial field theory is one such new approach. The standard model of particle physics assumes that all forces (fields) merge into one another (the primordial field) but has not yet shown this.

### 3. Physics of the Primordial Field

While QFT and general relativity are viewed as the supreme accomplishments of 20<sup>th</sup> century physics, they are incompatible, despite dozens of approaches to reconciling the two theories in loop quantum gravity. The establishment has invested a century of effort in these two theories, with many physicists investing decades in QFT and/or GR, creating a gigantic hurdle that new ideas must cross, typically with “push back” from the invested parties. Here we focus on explaining how and why primordial field theory produces fundamental results and do not focus on why QFT and GR have failed in this task.

Recall that Feynman coined the “*free lunch model*” as descriptive of a Big Bang, with negative gravitational energy exactly equal to the positive kinetic energy of expansion, yielding a total energy of zero. From the moment of creation until now, the density of the universe has decreased. We assume that, at earliest times, the mass energy density is as high as we wish it to be. Since Heaviside’s equations are mass-density-based and otherwise scale independent, we have access (at some point in time) to densities that lead to the “condensation” of particles from primordial field energy. Since we observe particle creation at LHC and CERN, we already know the region of energy density required to create particles. In fact, as primordial field theory was being developed circa 2006, physicists at LHC expected a “quark gas” to arise when heavy atoms were collided. Instead,

they found conditions that they described as a “perfect fluid”, exactly how we envision the primordial field. Thus, the ball of energy from two heavy nuclei colliding gives us a glimpse of the physically real primordial field.

Theories dealing with the creation and evolution of the universe are based on the turbulent explosion of a perfect fluid [8] and [9]. Characteristic of such turbulence is the formation of vortices, and their evolution (in many cases) into toroidal flows. Existence of the toroidal topology suggests analysis in terms of Calabi-Yau theory [10]. I invoke this theory because many relevant aspects of the problem can be formulated in terms of manifold proofs developed by Calabi and Yau, so that instead of making hypotheses I can state in terms of mathematical fact. I then derive the fermion’s half-integral spin in this context [11]. This approach leads to the possibility that the torus will *continue* shrinking until it reaches a non-physical infinite density at a point. Although the mass-gap existence theorem suggests this might occur, physical reality is based not solely on local mass, but also on the existence of charge for all fermions except neutrinos, which have a different (non-toroidal) structure [12].

Although fewer in number, other attempts to explain the origin of charge [13] and [14] typically introduce charge into equations in terms of the fine structure constant  $\alpha \sim e^2$ , or based on symmetries associated with the infinite dimensional expansions of quaternionic models. None that I am aware of address the *physical* reason for the existence of charge in the universe. In primordial field theory charge is potentially required to prevent the shrinking of the mass-based torus into an infinitely dense (chargeless) “point” particle. In the framework of duality, we obtain

$$\frac{\mathbf{v} \cdot \nabla \times \mathbf{B}}{|\mathbf{v}|^2} = \rho_q, \quad \frac{\mathbf{v} \cdot \nabla \times \mathbf{C}}{|\mathbf{v}|^2} = \rho_m. \quad (4)$$

Having formulated the creation of the fermion in primordial field theory, we now focus on creation of fractional charge, as required for quarks. The remainder of this paper treats this problem.

Formulating the particle in terms of Calabi-Yau, allows us to make use of the fact that Kähler manifolds provide 2D complex planes with  $a + ib$  representing the fact that  $a$  and  $b$  are orthogonal; multiplication of a vector (velocity) by duality operator  $i$ , supports orthogonal flows ( $\mathbf{C}$  and  $\mathbf{B}$ ) on the surface of the torus. In the complex formula,  $a + ib$ , the multiplication of vector  $a$  by imaginary  $i$  results in rotation of  $a$  by  $90^\circ$  in the plane. The duality operator  $-i$  rotates vector  $a$  by  $90^\circ$  in the opposite direction, while preserving its length. Examples are shown in **Figure 2**.

On a Kähler manifold, parallel-transporting a vector and then transforming it by the duality transformation is the same as duality transforming the original vector and then parallel-transporting it. Essentially, the C-field and its dual, the B-field, are *always* orthogonal and share the same parallel-transport properties.

In **Figure 2** the y-axis points locally in the direction of the core, circling the donut hole. The red C-field arrow,  $\mathbf{v}_C$ , has a component  $\mathbf{v}_{C_y}$  that circles the

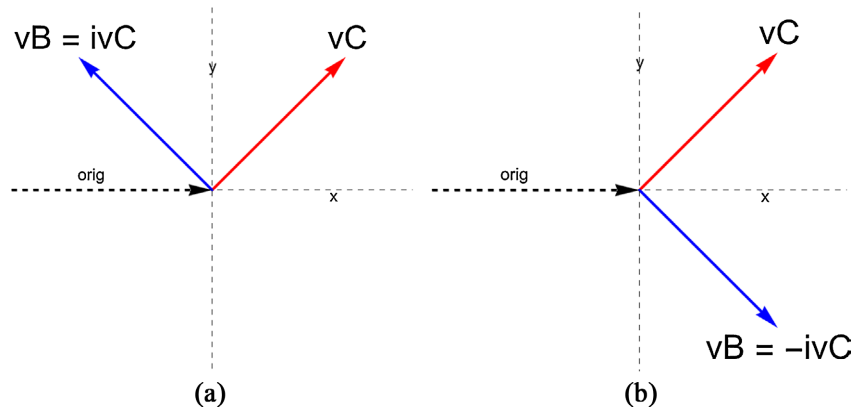


**Figure 2.** One can choose any point on the torus (Kähler manifold) as the origin. (a) If the C-field is tangent to the surface in the direction  $v_C$ , then the dual vector,  $v_B = iv_C$  is rotated by  $\pi/2$ , retaining its magnitude and tangential nature. (b) If the C-field is multiplied by  $-i = iii$  then the dual vector,  $v_B = -iv_C$  is rotated by  $3\pi/2$  or  $-\pi/2$ .

donut hole and another  $v_{C_x}$  that circles the torus. In **Figure 2(a)** the blue B-field arrow,  $v_B = iv_C$ , has a component  $v_{B_y}$  that circles the donut hole in the same direction as the C-field, and another  $v_{B_x}$  that circles the torus in the direction opposite to  $v_{C_x}$ . In **Figure 2(b)** the blue B-field arrow,  $v_B = -iv_C$ , has a component  $v_{B_y}$  circling the donut hole opposite to the C-field, while  $\vec{v}_{B_x}$  circles the torus in the same direction as  $v_{C_x}$ . Both C-field and B-field perform a  $U(1) \times U(1)$ -rotation on the torus requiring that two  $2\pi$ -rotations are required to return to the original state at the starting point, which can be any point on the torus. The Chern class vanishes, so there is no point on the manifold that will halt flow; the C-field and its dual, the B-field, flow endlessly in this stable, self-organized field-structure.

The mass of the field energy flowing around the hole gives rise to angular momentum with differences proportional to  $C_\theta \cdot C_\theta \pm B_\theta \cdot B_\theta$ . If the system with greater inherent angular momentum is more stable than one with less angular momentum, then the electron may be inherently more stable than the positron and may account for the (still unexplained) predominance of electrons over positrons in our universe.

We can approach the problem purely mathematically, but we choose a visual proof based on a *Mathematica* Demonstration project titled “torus made from coiling triangles”, as shown in **Figure 3**.

The torus surface is filled with triangles. A black line along one edge of one triangle is extended to follow the edge of an adjacent triangle that joins the first triangle at a vertex. Continuing this action traces out a line that wraps around the torus, like a path in the C-field flow. Next, several red lines are drawn along appropriate triangle edges that cross the black line, representing B-field flow that is neither parallel nor orthogonal to the C-field flow.

#### 4. Fractional Fermionic Charge

In **Figure 3** we trace an edge of the triangles and imagine that this represents

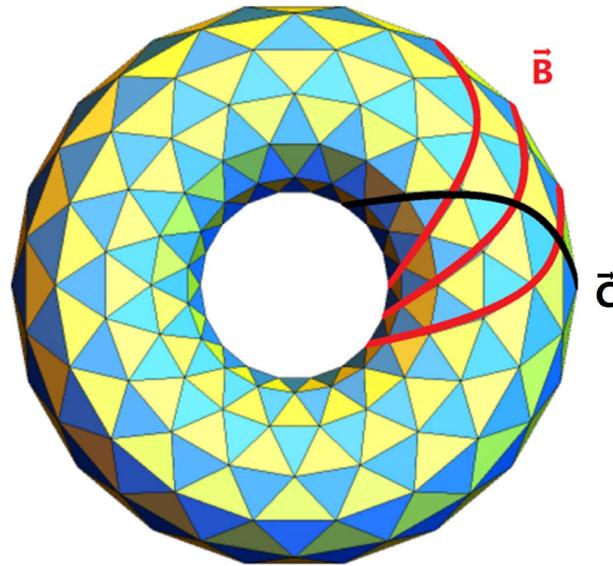


**Figure 3.** “Torus made from coiling triangles” —A Wolfram Demonstration project.

C-field flow around the torus. If we then trace another edge over several relevant triangles and assume that this image represents a B-field flow around the torus, we see clearly that these two flows are not orthogonal (corresponding to  $b = ia$ ), yet they appear to represent piece-wise continuous paths around the torus. Since the triangles appear to be equilateral, the angle between the black and red lines is about  $60^\circ$  and the value of  $\mathbf{B} \cdot \mathbf{C} = 0.5$ . If C-field flow is the adjacent side and B-field flow is the hypotenuse, the C-field is  $\frac{1}{2}$  the B-field or the B-field path is twice the C-field path. This implies that if the C-field flow returns to its starting point (any point on the surface of the torus) in  $4\pi$  then the B-field (at  $60^\circ$  with respect to the C-field) will return to its starting point in  $8\pi$ .

If this is the case, the B-field winds around the torus twice as fast as the C-field, given the same rate  $d\theta/dt$  where  $\theta$  is the angle around the donut hole. If the two fields begin and end at the same point, then

$(d\phi/dt)_B = 2(d\phi/dt)_C$  where  $\phi$  is the angle of rotation around the torus (orthogonal to  $\theta$ ). That is, the B-field circles the torus at twice the angular velocity as the C-field. Key is that non-orthogonal angles should be considered, and this leads us to consider the angle  $70.53^\circ$ , such that we find  $\mathbf{B} \cdot \mathbf{C} = 0.33333$ . Summarizing these three cases:

$$\mathbf{B} \cdot \mathbf{C} \sim \cos(60^\circ) = \frac{1}{2}, \quad \mathbf{B} \cdot \mathbf{C} \sim \cos(70.53^\circ) = \frac{1}{3}, \quad \mathbf{B} \cdot \mathbf{C} \sim \cos(90^\circ) = 0 \quad (5)$$

The projection of  $\mathbf{C}$  flow onto  $\mathbf{B}$  is zero for the orthogonal case, and one-half and one-third for the non-aligned flows (which is not to say non-correlated.) Thus, while the C-field winds around the torus twice for one rotation around the hole in the torus, the  $60^\circ$ -case winds around twice as often as the C-field, and the  $70.53^\circ$ -case winds around three times for each C-field winding.

The tangent vectors that we have generated in our Kähler manifold correspond

to velocities, which we have resolved into  $v_\theta$  and  $v_z$  where  $v_\theta$  represents the flow of the field around the donut hole and  $v_z$  represents the flow of the field through the donut hole.

Our toroidal model evolved based on the circulation of the C-field in the  $U(1) \times U(1)$ -symmetry of the structure. In our development of discrete charge, we chose to make the  $\mathbf{B}$  and  $\mathbf{C}$ -fields orthogonal and use of Calabi-Yau theory showed that if the two flows start at the same point, they will return to the same starting state after parametrically traversing  $4\pi$ .

For non-orthogonal flows, the goal is having each field return to the same state at the same time and place, however, multiple windings complicate the picture.

The C-field is the basis of the toroidal structure evolving in the ultra-dense primordial field, and thus the behavior of the C-field is fundamental. In order to preserve  $\text{spin} = \frac{1}{2}$ , the C-field will continue to traverse a  $4\pi$ -parametric path before cycling. Repetition of this basic cycle should occur essentially “forever” (or until an interaction of sufficient energy disrupts the cycle).

In this case the B-field winds around the torus at the same rate as the C-field, but in an orthogonal direction. In our current situation the B-field winds around the same torus either two or three times for the C-field’s one cycle. What this means is that the B-field will pass through the donut hole in the torus two or three times for each C-field pass. On the other hand, the B-field must match the C-field in the sense that both must return to the starting state after the C-field executes a  $4\pi$  cycle. Thus the  $n > 1$  winding of the B-field will require that the B-field passes through the hole faster than the C-field, such that,  $\left(\frac{d\phi}{dt}\right)_B > \left(\frac{d\phi}{dt}\right)_C$ . But in order to reach the same final state (= initial state) for each field, the B-field must rotate about the hole more slowly than the C-field, thus  $\left(\frac{d\theta}{dt}\right)_B < \left(\frac{d\theta}{dt}\right)_C$ . Specifically, for  $n$  B-field windings ( $n = 1, 2, 3$ ), we write:

$$\left(\frac{d\phi}{dt}\right)_B = n \left(\frac{d\phi}{dt}\right)_C \quad (6)$$

and

$$\left(\frac{d\theta}{dt}\right)_B = \frac{1}{n} \left(\frac{d\theta}{dt}\right)_C \quad (7)$$

Finally, we note that  $\theta$  and  $\phi$  are not independent but are correlated over a closed path so that each completes an integral number of  $2\pi$  rotations at exactly the same time and place. For  $n = 1$  this correlation satisfies

$$\left(\frac{d\theta}{dt}\right)_B \left(\frac{d\phi}{dt}\right)_B \equiv \left(\frac{d\theta}{dt}\right)_C \left(\frac{d\phi}{dt}\right)_C \quad (8)$$

We now generalize this for integer winding number  $n$ :

$$\left(\frac{d\theta}{dt}\right)_B \left(\frac{d\phi}{dt}\right)_B \equiv \frac{1}{n} \left(\frac{d\theta}{dt}\right)_C n \left(\frac{d\phi}{dt}\right)_C \quad (9)$$

In other words,  $\theta\phi$ -correlation of the B-field over  $n$   $4\pi$ -cycles is identical to  $\theta\phi$ -correlation of the C-field over a  $4\pi$ -cycle. If these topological windings of the B-field are related to the electric charge current producing the B-field, then we have 1, 2, and 3 units of charge  $q$  corresponding to 1, 2, and 3 windings, compatible with the solenoidal picture relating the number of windings to the induced field. If the charge of the electron is 1, this corresponds to three elemental units of charge associated with one C-field winding; the other two cases correspond to 1 and 2 such elemental charges. These are the charges assigned to *down* quarks and *up* quarks, respectively, so our fermion model incorporates the charges for both electrons and quarks in the standard model.

Table of fermions

fermion	$q$	charge
e	$\frac{3}{3}$	$-e$
u	$\frac{2}{3}$	$\frac{+2e}{3}$
d	$\frac{1}{3}$	$\frac{-e}{3}$

“*The Origin of Electric Charge in Quantum Gravity*” [15] includes anti-particles, and, although attempting to explain the origin of charge, assuming that only a single charge existed, we now see that *three charges can exist based on the same theory*, if the electron corresponds to three windings compared to two for the up quark and one for the down quark. The same reasoning about relative directions of the fields applies, thus yielding positive and negative charges: particles and anti-particles.

## 5. Charge-Based “Shrinkage” of Fermions

The duality of gravitomagnetism and electromagnetism is derived from primordial field theory. A significant aspect of this analysis dealt with “shrinkage” of the torus associated with gravitomagnetic structure. Why assume that the torus is shrinking? In our mass gap existence theorem, we calculate the interaction of higher-order self-induction on a fractal lattice. Past a certain threshold, the forces are attractive and point to the center of the torus, causing the torus to shrink. This is characteristic of the self-interaction, and we expect it to continue unless and until it is terminated. If at some point the scale is such that the gravitomagnetic and electromagnetic scales and forces are compatible (Equation (4)), then we expect the dual entities to exist. If this is the case, we focus on the physics involved:

For the C-field we assume conservation of angular momentum, and as a consequence, the torus spins faster as its radius shrinks, preserving angular momentum but increasing mass density, based on  $mv'r' = mvr$ . If the radius  $r$  of the

torus is shrinking, then  $r' = r - dr$  and  $v' = v \left( \frac{r}{r - dr} \right)$ . For the B-field Coulomb's law, derived from experiment,  $F \propto \frac{q_1 q_2}{d^2}$  describes the force between two electric charges,  $q_1$  and  $q_2$ , separated by distance  $d$ , which in our case is  $2r$ , where  $q_1$  is a portion of charge on the torus and  $q_2$  another on the opposite side of the torus. Since  $d = 2r$ , if the torus shrinks by  $r' = r - dr$  then the force varies according to:  $d^2 \Rightarrow 4r^2 - 4rdr + (2dr)^2$ . Ignoring the second order differentials this force then becomes  $F \propto \frac{(q_1)^2}{r^2 - rdr}$  where we set  $q_1 = q_2$  and ignore the constant factor of 4 in the denominator. Thus, if the radius of the torus shrinks by  $dr$  then the repulsive force between the charges on opposite sides of the torus increases as shown; self-repulsion of the charge on the torus opposes shrinkage of the particle. In the limit  $r \rightarrow dr$ , the repulsive force becomes infinite, thus the shrinkage will terminate due to charge before this occurs.

A first response might be that “*the electrical force is about  $10^{39}$  times stronger than the gravitation force*”. But we are not counting on the gravitational force  $F = mG$  to “pull the particle together”. Instead, consider the gravitomagnetic forces that we have assumed in our derivation of the mass gap existence theorem, specifically,  $F = mv \times C$ . Primordial field theory derives Heaviside's relation  $\nabla \times C \sim \rho v$  and  $C = r \times \rho v$ . We assume speed  $v$  is on the order of the speed of light  $c$ , and the force of the C-field is proportional to density. The local density at the Big Bang is assumed as high as we wish it to be, so the force exerted by the C-field on the mass of the torus is effectively unlimited; that the gravitational force is  $\sim 10^{39}$  stronger than the gravitational force  $mG$  is no longer the most relevant factor. Recall that the enormous repulsive force between protons in a nucleus must be more than compensated for by a strong nuclear force. We are not at the moment investigating the nuclear force, but neither are we investigating the gravitational force  $F = mG$ .

The self-repulsion of electric charge is considered to terminate the shrinkage of the toroidal fermion; this is dependent on the amount of charge, which we now see is proportional to winding number. Thus, discrete winding numbers 1, 2, 3 are associated with discrete electric charge  $q$ . We conclude that the electron, with charge  $q$ , has the greatest charge and will terminate the shrinkage of the fermion before the quark charges do so. In similar fashion the up quark, with charge  $2q/3$ , will cease shrinking before the down quark, with charge  $q/3$ . That is, the electron is the largest particle (toroidal radius) with the up quark next, then the down quark is smallest, as shown in **Figure 4**. These relations follow from ontological reasoning about the *condensation* of fermions from ultra-dense gravito-magnetic turbulence.

The shrinkage (pre-charge) and conservation of angular momentum implies that the shrunken fermion has faster rotational velocity and effectively spins faster! This brings into account the fact that [16] spin has, or is equivalent to, mass. As a consequence, the smaller the spinning particle (**Figure 5**) the faster it spins

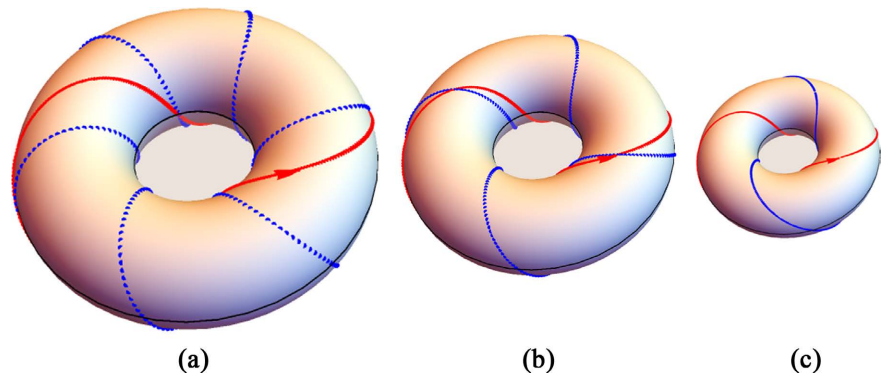


**Figure 4.** Relative quark sizes and charges. (a) The electron, with three B windings (blue) for one C-winding (red) has the greatest charge and thus terminates shrinkage first. (b) The up quark, with two B-windings per C-winding terminates shrinkage next. (c) The down quark, with one B-winding per C-winding, terminates last, hence is the smallest of the charged particles.

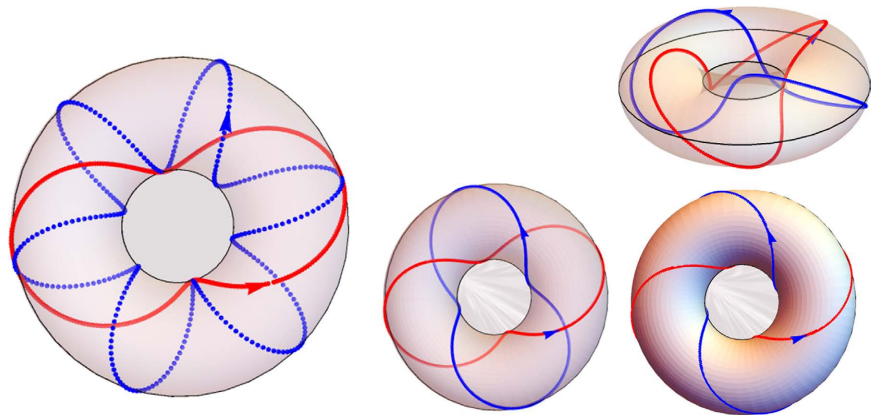


**Figure 5.** Translucent electron and quark topologies and relative scales, showing complete paths on vortex manifold.

and the more associated mass it has.

Summarizing, the electron is the largest fermion but has the lowest mass: the down quark is the smallest, densest (fastest spinning) with the highest mass; the up quark mass is between that of the electron and the down quark. The mass of the electron is 0.511 MeV. While quark masses are unknown, they have recently been assigned the values 2.1 MeV and 4.79 MeV on the basis of the charm quark mass, which is about 500 times more massive and hence easier to determine, using ratio-based analysis [17]. These facts align with our predicted properties, and, to my knowledge, the above development is the first to derive quark charges, relative quark sizes, and relative quark masses, in a manner also compatible with the derivation of electrons.

## 6. The Significance of Measurements on a Model

We have noted that most attempts to explain the origin of charge are mathematical, for example, Faber's addition of the fine structure constant  $\alpha \sim e^2$  to the Lagrangian. There is no attempt to explain physically how charge originates. In

contrast, we have assumed extreme local turbulence which generates vortices and, often, toruses (tori). Once a torus exists, we analyze it physically by applying conservation laws to  $U(1) \times U(1)$  flows on the toroidal surface. In other words, the physics is not *built into* the torus, but is *applied to* the torus. We begin with a torus since we know that turbulence produces the toroidal construct. Based on our extensive experience with electromagnetic fields created by charge flow, we have constructed solenoidal tori, driven by current flowing through the solenoidal coils, and we also measure helical flow around a locally linear charge flow. Flowing fields have energy density and hence mass density, and flowing mass induces gravitomagnetic circulation about the flow. This induced field then induces a secondary circulation, which in turn produces a tertiary circulating flow, and these higher order induced fields interact with each other. The interaction is shown to reach a stabilizing region or zone leading to a finite mass, and hence a mass gap between this mass and the vacuum state. This analysis tells us that toroidal flows endure, as observed in smoke rings and even air rings in water, produced and played with by porpoises. According to Dyson [18], Maxwell was extremely enthusiastic about a vortex model of molecules founded on Helmholtz's hydrodynamics, showing that "*in a perfect fluid, such a whirling ring, if once generated, would go on whirling forever*"—perfect for fermion behavior.

Based on the known existence of toroidal flows, and the calculation of higher order self-interaction of the gravitomagnetic induced circulation, we derived the mass gap existence theorem in terms of a fractal-lattice-based calculation and investigated the angular momentum or spin, if any, associated with enduring toroidal flow. To do so we employed Calabi-Yau theory and specifically Kähler manifolds, vanishing Chern class, and Ricci curvature. The result of this Calabi-Yau based analysis is half-integral quantized spin, characteristic of fermions. Let us now distinguish between the mathematics and the physics of this model of electric charge. Physically, we know from Heaviside equations, the gravitomagnetic field circulates helically with  $U(1)$  symmetry ( $e^{i\theta}$ ). Nevertheless, when bent or wrapped around on itself to form a torus the resulting  $U(1) \times U(1)$  symmetry is difficult to relate precisely to Heaviside equations.

In fact, at this point we revert to pure mathematics, sans physics for the moment. In other words, the torus is a mathematical construction based on parameters, and in order to calculate surface flow, we use the parametric equations to generate tangential velocity vectors on the Kähler manifold associated with the toroidal flow. This is the key point being made here; calculation of the closed flow path on the surface of the torus is done based on the parametric model, *not* on physics. That is, we physically justify the existence of the torus, then we switch to pure math to parametrically calculate flow velocity, for animated display of a tangent vector being transferred along a closed path on the toroidal surface. It is this calculation that leads to the half-integral spin associated with the  $U(1) \times U(1)$  surface flow.

At this point we re-integrate physics by integrating momentum conservation relations differentiating flow *through* the hole in the torus and flow *around* the hole in the torus. Thus we impose physical conservation laws as constraints on the mathematical paths that result from a parametric treatment of the torus in terms of velocity vectors along a closed path.

The animation of the model runs indefinitely, effectively forever, which is what *is* desired for fermion behavior, yet the model is derived mathematically, subject to physical constraints. The physics of the analysis resolves the flow through the donut hole in terms of energy-momentum conservation analysis of the flow of the field around the donut hole.

That is, we physically justify consideration of the torus and mathematically calculate flow vectors based on the parametric definition of a torus. Then physical energy based reasoning is applied to derive each  $U(1)$ -based flow present in the  $U(1) \times U(1)$  symmetry, ending up with the physics based equation:

$$v = \sqrt{v_\theta^2 + v_z^2} \tag{7}$$

Does this physics-derived equation match the parametrically derived velocity exhibited in the dynamic model? To answer this, we make measurements on our dynamical model and compare to the prediction of the physics model. Since these calculations being measured are based on the parameters of the torus, we display key parameters in **Figure 6**.

This was first done in the Calabi-Yau paper in **Table 1**.

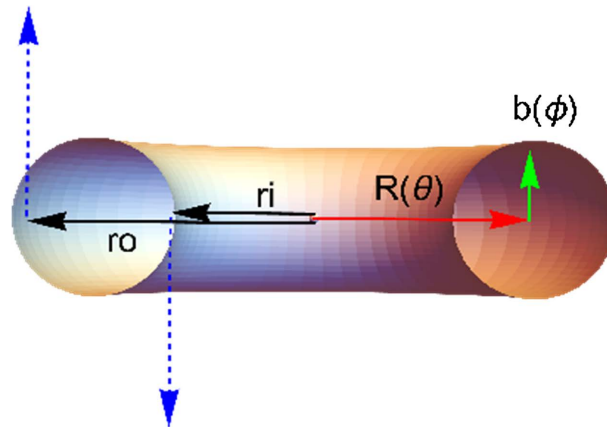


**Figure 6.** Cartoon depicting relevant vectors of the torus model of the fermion. The radii  $r_i$ ,  $r_o$ , and  $R$  used in measurements in **Table 1**.

**Table 1.** Measurement of velocity components

deg	0	30	60	90	120	150	180	210
$v_\theta$	10.8	9	10.8	3	10.8	9	10.8	3
$v_z$	0	9	0	9	0	9	0	9
$v$	10.8	12.7279	10.8	9.48	10.8	12.72	10.8	9.48
radi	$R$	$r_o$	$-R$	$-r_i$	$R$	$r_o$	$-R$	$r_i$

At any point on the manifold the velocity  $\mathbf{v} = \mathbf{v}_\theta + \mathbf{v}_z$ . If we square both sides, term  $\mathbf{v}_\theta \cdot \mathbf{v}_z = 0$  since  $\vec{v}_\theta$  and  $\vec{v}_z$  are orthogonal, hence again  $v = \sqrt{v_\theta^2 + v_z^2}$ . For example, at  $30^\circ$  the velocity is  $\sqrt{9^2 + 9^2} = 12.7279220$  while at  $90^\circ$   $v = \sqrt{3^2 + 9^2} = 9.48$ . We see from the table that the measurements confirm the intuitively derived relations based on the reasoning about *conservation of momentum*. In short, the dynamic visualization of the field behavior intuitively confirms the correctness of the model/theory, while the measurement access to arbitrary parameters can serve as proof of the flow model worked out by conservation equations and the  $U(1) \times U(1)$ -symmetry. Measurements on the model agree in detail with intuitively and/or analytically derived behavior. New results in this paper are based on fractional charge, represented by integer-based windings. Since our original model exhibited half-integral spin with  $4\pi$ -rotation over the closed path, the model with  $n = 2$  windings will travel from  $\theta = 0$  to  $\theta = 8\pi$ , before reaching its starting point.

The relevant table of measurements associated with this  $n = 2$  case is given in **Table 2**.

When these measurements are checked against Equation (7), we find  $\sqrt{9^2 + 12^2} = 15$  and  $\sqrt{13.42^2 + 0^2} = 13.42$  and  $\sqrt{3^2 + 12^2} = 12.36$ , in complete agreement with the table. Note that, although we made measurements up to and including  $8\pi$ , the measurements in **Table 2** repeat, such that if we extended the table the next column corresponding to  $4\pi$  (at  $180^\circ$ ) would reproduce the column labelled zero degrees, followed by each column of **Table 2** until we reach  $8\pi$  at  $360^\circ$ . Thus, we see that the measurements performed on the 2-winding case agree exactly with the values predicted by the relevant physics.

Finally, we consider the case for  $n = 3$  windings.

**Table 2.** Measurement of  $n = 2$  velocity components.

deg	0	24	46	68	91	114	136	158
	0		$\pi$		$2\pi$		$3\pi$	
$v_\theta$	13.42	9	13.42	3	13.42	9	13.42	3
$v_z$	0	12	0	12	0	12	0	12
$v$	13.42	15	13.42	12.36	13.42	15	13.42	12.36
radi	$R$	$r_o$	$-R$	$-r_i$	$R$	$r_o$	$-R$	$r_i$

**Table 3.** Measurement of  $n = 3$  velocity components.

deg	0	16	30	45	60	75	90	105
	0		$\pi$		$2\pi$		$3\pi$	
$v_\theta$	18.97	9	18.97	3	18.97	9	18.97	3
$v_z$	0	18	0	18	0	18	0	18
$v$	18.97	20.12	18.97	18.25	18.97	20.12	18.97	18.25
radi	$R$	$r_o$	$-R$	$-r_i$	$R$	$r_o$	$-R$	$r_i$

Again, if this table is extended to  $12\pi [(n=3)*(4\pi)]$  the same numbers repeat, with nothing new showing up, so there is no information to be gained by this extension. For **Table 3** the key values satisfy  $\sqrt{18.97^2 + 0^2} = 18.97$  and  $\sqrt{9^2 + 18^2} = 20.12$  and  $\sqrt{3^2 + 18^2} = 18.25$ . Not represented in **Table 3** are several other measurements taken *between* the columns, for example,  $\sqrt{17.3^2 + 9^2} = 19.5$  and  $\sqrt{16.225^2 + 9^2} = 18.55$ , both of which satisfy the physics-derived velocity equation.

In summary, the dynamic model of surface flow, generated parametrically, runs “forever” as *required* for a model fermion. Physical analysis of the flow, based on momentum-energy conservation, leads to velocity predictions that are checked against the parametric behavior and found to be in perfect agreement. This sufficient proof of the quark model allows us to continue with our analysis of quark properties.

While we have derived this relative information from ontological reasoning, observe that we have not derived the “color” associated with individual quarks; there is nothing in our derivation that points to color as an inherent property of quarks. One might assume that color rises in quark interactions, which we have not yet considered. Another aspect of charge creation that we have glossed over is conservation of charge. We have, for electrons and quarks, explained the creation of charge associated with a gravitomagnetic induced/condensed particle with toroidal structure. That is, our primordial field model has ontologically explained aspects of particles that have not heretofore been recognized, but there are still associated questions to be resolved. Each of these issues, color and conservation of charge will be handled in a future paper.

## 7. Comparison with Other Theories of Quarks and Electrons

How does this theory compare with other treatments, such as Nilsen’s theory of the relationship between quarks and electrons, mentioned in the introduction? He claims that the quarks can be expressed as charge equalization of the electron but fails to define “charge equalization”: “Based on the current Standard Model, there is no way to build any of the two charges of quarks, equaling  $1/3$  and  $2/3$ .” “Although quarks are less charged than the electron, the masses are larger. The up-quark has a mass in excess of four electrons and the down-quark in excess of nine electrons.” He does not explain this, nor is it explained in any other theory of which the author is aware, but we note that the relation to the square of the winding numbers of the separate fermions offers an apparent correlation that will be addressed in future work. In Nilsen’s hypothesis a “confinement of three charge oppositions” is described. The third opposition is named the *triotron*. This particle appears to be introduced based on a need to derive fractional charge relations, as opposed to any ontological derivation. Similarly, his “charge oppositions” are considered as a three dimensional vibration, otherwise undescribed and unjustified. Via the unexplained introduction of these concepts, he derives fractional charges  $1/3$  and  $2/3$ , as needed for quarks, but this treatment

leads to the interpretation of the proton as consisting of 17 elementary charges and his neutron consists of 22 elementary charges. In short, the addition of a proposed triotron, never seen and with no ontological or physical justification, is plugged into an equally unexplained formula for “charge equalization” in terms of the number of dimensions  $D$ , the number of elementary charges  $E$ , and the number of counter phases  $C$  (also undefined and unexplained). He claims that the *triotron* can annihilate both electrons and positrons, and currently cannot be measured.

In contrast to the above, based on almost universal agreement that all forces merge at the moment of creation, and developing the self-interaction equation governing this primordial field, the author has constructed a theory based on this ontology that immediately leads to a quantum theory of gravity consistent with Heaviside’s gravitomagnetic equations and equivalent to Einstein’s general relativity, but without the associated paradoxes and century old mysteries. This quantum gravity theory is then used to extend the Yang-Mills theory to prove a mass-gap existence theorem and then extended to Calabi-Yau (much of the mathematical basis of string theory) to derive one-half integral spin. These concepts, developed logically and with ontological consistency present nowhere else, are then extended in terms of  $N$ -windings on the hyper-dense gravitomagneto fluid-based physical manifold, to show that the heretofore unexplained fractional charges fall out of this treatment, without any ad hoc introduction of new particles, new undefined terms, or such, and with no apparent paradoxes, with which other theories are replete.

Another theory mentioned in the introduction, suggested by a reviewer to be relevant to primordial field theory of quantum gravity, is Tejinder Singh’s theory of ‘Spontaneous Quantum Gravity’, in which the failure of classical physical entities to exist in two different places at once is supposed to be explained by extension of the Ghirardi, Rimini, Weber, and Pearle (GRWP) theory of “spontaneous collapse” of the quantum mechanical wave function, an ad hoc hypothesis with no other reason for existing except that it supposedly “solves” the problem of “collapse of the wave function”, a formulation that many physicists no longer view as a real problem. If one does view this as a problem, and views the GRWP hypothesis as a reasonable, if ad hoc, solution to the problem, then Singh’s extension to “quantum gravity” should be deemed appropriate, but this has no relation to the problem of the origin of quarks in quantum gravity, which is the topic of this paper.

## 8. Summary and Conclusion

According to Wiki (Quantum Gravity): “The current understanding of gravity is based on Einstein’s general theory of relativity, which incorporates his special theory of relativity and deeply modifies the understanding of concepts like time and space.” Yet GR has limitations: “the gravitational singularity inside of black holes, the ad hoc postulate of dark matter, as well as dark energy, and its relation

to the cosmological constant are among the current unsolved mysteries regarding gravity.” Elsewhere I analyze the ontology of energy-time theory compared to space-time theory, finding that Galilean covariance is compatible with time dilation but not length contraction and that such mysteries as quasi-local mass are explained by primordial field theory. The assumption in GR is that Heaviside is a weak field approximation to relativity and is thus insignificant at particle scales. The focus on geometry has blinded the community to the density-based scale-independent Heaviside theory that is both derived from and iteratively converges to relativity. The fact that local energy density is not definable (specifically prohibited!) in curved spacetime (explained in [19]) has convinced many that local density-based gravitational energy is not worth spending time thinking about. In fact, Feynman, Weinberg, and others have stated that geometry in curved spacetime is absolutely unnecessary for description of gravity.

We have shown that the primordial field theory leads to Heaviside gravitomagnetism and its dual, Maxwellian electromagnetism, and the assumption of ultra-dense gravity at the big bang and in LHC atomic collisions leads to an ontological derivation of:

- Fermion mass-gap [Yang-Mills]
- $\frac{1}{2}$ -integer spin [Calabi-Yau]
- Discrete charge [winding number]
- Discrete magnetic moment [proportional to spin]
- Relative fermion masses and sizes based on charge.

*No other theory of quantum gravity even attempts to derive such results!*

In considering Primordial Field Theory versus QED and QCD, one is faced with trading off years, even decades, of investment in GR with its unsolved mysteries for a novel approach to quantum gravity that appears to be paradox-free and offers solutions to otherwise unsolved mysteries. The tradeoff, of course, must be answered by each physicist. By deriving relevant and relative properties of fermions, electrons and quarks, primordial field theory has apparently surpassed all other forms of quantum gravity and further development of Hadron physics will yield even greater understanding. And despite the inherent bias in its training, artificial intelligence such as GPT-4o accepts the assumptions, the logic, and the math of primordial field theory. Such AI acceptance, I believe, will soon force establishment physicists to come to the same conclusion.

## Conflicts of Interest

The author declares no conflicts of interest regarding the publication of this paper.

## References

- [1] Armas, J. (2021) *Conversations on Quantum Gravity*. Cambridge U Press.

- 
- [2] Nilsen, I. (2022) On the Relationship between Quarks and Electrons. *Journal of High Energy Physics, Gravitation and Cosmology*, **8**, 681-689. <https://doi.org/10.4236/jhepgc.2022.83050>
- [3] Singh, T.P. (2021) Spontaneous Quantum Gravity. *Journal of High Energy Physics, Gravitation and Cosmology*, **7**, 880-905. <https://doi.org/10.4236/jhepgc.2021.73050>
- [4] Klingman, E.E. (2022) Particle Creation from Yang-Mills Gravity. *Journal of Modern Physics*, **13**, 1128-1145. <https://doi.org/10.4236/jmp.2022.137065>
- [5] Jefimenko, O. (2000) Causality, Electromagnetic Induction & Gravitation. 2nd Edition, Electret Scientific Co.
- [6] Heaviside, O. (1893) A Gravitational and Electromagnetic Analogy. *The Electrician*, **31**, 81-88.
- [7] Zee, A. (2003) Quantum Field Theory in a Nutshell. Princeton Univ. Press.
- [8] Volovik, G. (2003) The Universe in a Helium Droplet. Oxford University Press.
- [9] Svistunov, B.V., Babaev, E.S. and Prokofev, N.V. (2021) Superfluid State of Matter. CRC Press.
- [10] Yau, S. (2010) The Shape of Inner Space. Basic Books.
- [11] Klingman, E.E. (2024) Calabi-Yau Topology of Primordial Fermions. *Journal of Modern Physics*, **15**, 132-158. <https://doi.org/10.4236/jmp.2024.151005>
- [12] Klingman, E. (2021) A Self-Stabilized Theory of Neutrinos. *Journal of High Energy Physics, Gravitation and Cosmology*, **7**, Article No. 3.
- [13] Faber, M. (2012) Particles as Stable Topological Solitons. *Journal of Physics: Conference Series*, **361**, Article ID: 012022. <https://doi.org/10.1088/1742-6596/361/1/012022>
- [14] Van Leunen, H. (2015) On the Origin of Electric Charge. *Open Access Library Journal*, **2**, 1-14.
- [15] Klingman, E.E. (2024) The Origin of Electric Charge in Quantum Gravity. *Journal of Modern Physics*, **15**, 511-535. <https://doi.org/10.4236/jmp.2024.154025>
- [16] Smith, J., *et al.* (2018) Rotational Energy as Mass in  $H_3^+$  and Lower Limits on the Atomic Masses of D and  $^3\text{He}$ . *Physical Review Letters*, **120**, Article ID: 143002.
- [17] Cho, A. (2010) Mass of the Common Quark Finally Nailed down. <https://www.science.org/content/article/mass-common-quark-finally-nailed-down>
- [18] Dyson, F.J. (2007) Why Is Maxwell's Theory So Hard to Understand? *2nd European Conference on Antennas and Propagation (EuCAP 2007)*, Edinburgh, 11-16 November 2007. <https://doi.org/10.1049/ic.2007.1146>
- [19] Klingman, E.E. (2022) A Re-Interpretation of Quasi-Local Mass. *Journal of Modern Physics*, **13**, 347-367. <https://doi.org/10.4236/jmp.2022.134025>